Cooling the Collective Motion of Trapped Ions to Initialize a Quantum Register

B. E. King,* C. S. Wood, C. J. Myatt, Q. A. Turchette, D. Leibfried,† W. M. Itano, C. Monroe, and D. J. Wineland
Time and Frequency Division, National Institute of Standards and Technology, Boulder, Colorado 80303
(Received 6 March 1998)

We report preparation in the ground state of collective modes of motion of two trapped $^9Be^+$ ions. This is a crucial step towards realizing quantum logic gates which can entangle the ions' internal electronic states. We find that heating of the modes of relative ion motion is substantially suppressed relative to that of the center-of-mass modes, suggesting the importance of these modes in future experiments. [S0031-9007(98)06838-0]

PACS numbers: 03.67.Lx, 03.65.–w, 32.80.Pj

In physics, quantum computation [1] provides a general framework for fundamental investigations into subjects such as entanglement, quantum measurement, and quantum information theory. Since quantum computation relies on entanglement between qubits, any implementation of a quantum computer must offer isolation from the effects of decoherence, but also allow controllable and *coherent* interaction between the qubits. Cirac and Zoller [2] have proposed an attractive scheme for realizing a quantum computer, which is scalable to an arbitrary number of qubits. Their scheme is based on a collection of trapped atomic ions, where each qubit (one per ion) is comprised of a pair of the ions' internal states, while quantum information is transferred between different ions using a particular quantized mode of the ions' collective motion. This "quantum data bus" must first be initialized in a pure quantum state [2]: for example, its ground state [3]. The basics of this scheme have been demonstrated experimentally in a fundamental logic gate (a Controlled-NOT) operating between a motional mode of a single trapped ion and two of the ion's internal states [4]. In that work, the motional state was initialized in the ground state by laser cooling [5]. The next step towards implementing the Cirac-Zoller scheme is to cool at least one mode of collective motion of multiple ions to the ground state. In this Letter, we describe the first experiments to realize this goal. We also report a significant difference between the decoherence rates of the center-of-mass and non-center-of-mass modes of motion.

We confine $^9Be^+$ ions in a coaxial-resonator-based rf (Paul) trap, similar to that described in Ref. [6]. The electrodes in this trap are made from 125-μm-thick sheets of Be metal, as shown in Fig. 1. We apply a potential $\phi(t) = V_0 \cos(\Omega_T t) + U_0$ to the (elliptical) ring electrode relative to the end cap electrodes. If several ions are trapped and cooled, they will naturally align themselves along the major axis of the ring electrode. The electrode's elliptical shape, in combination with $U_0 > 0$, allows a linear crystal to be maintained while suppressing rf micromotion of the ions along this direction [7]. With $V_0 \approx 520$ V, $\Omega_T/2\pi \approx 238$ MHz, and $U_0 = 0$ V, the pseudopotential oscillation frequencies are $(\omega_x, \omega_y, \omega_z)/2\pi \approx (4.6, 12.7, 17.0)$ MHz. With $U_0 = 18.2$ V, the frequencies become $(8.6, 17.6, 9.3)$ MHz. Figure 1 shows two ions confined in the trap and imaged with an $f/3$ lens system onto a position-sensitive photomultiplier tube.

The ions are cooled and probed with laser beams whose geometry is indicated in Fig. 2(a). The relevant level structure of $^9Be^+$ is shown in Fig. 2(b). The quantization axis is defined by an applied static magnetic field; $|\boldsymbol{B}| \approx 0.2$ mT. The levels of interest for quantum logic operations are the $2s\,^2S_{1/2}|F = 2, m_F = 2\rangle$ and $2s\,^2S_{1/2}|F = 1, m_F = 1\rangle$ states, abbreviated by $|{\downarrow}\rangle$ and $|{\uparrow}\rangle$, respectively. Laser beams D1, D2, and D3 are σ^+ polarized and focused to nearly saturate the ions ($I_{sat} \approx 85$ mW cm^{-2}). Beams D1 and D2 provide Doppler precooling in all three dimensions, and beam D3 prevents optical pumping to the $|F = 2, m_F = 1\rangle$ state. The $|{\downarrow}\rangle \rightarrow 2p\,^2P_{3/2}|F = 3, m_F = 3\rangle$ transition (radiative linewidth $\gamma/2\pi \approx 19.4$ MHz), driven by D2, is a cycling transition, which allows us to detect the ion's electronic state ($|{\downarrow}\rangle$ or $|{\uparrow}\rangle$) with nearly unit detection efficiency.

Beams R1 (σ^+/σ^- polarized) and R2 (π polarized) are used to drive stimulated Raman transitions between

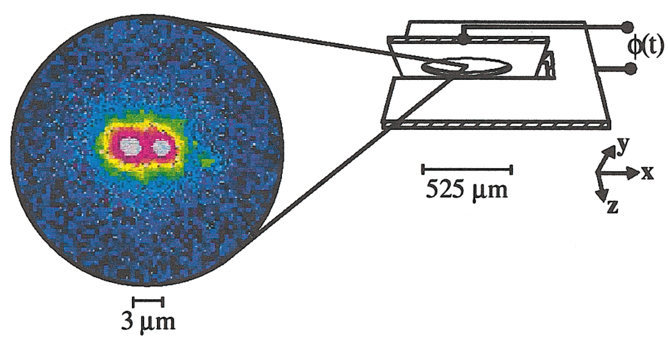

FIG. 1(color). Two ions trapped in an elliptical rf (Paul) trap. The ring has an aspect ratio of 3:2 and the major axis is 525 μm long. The slot which forms the end caps is 250 μm across. A potential $\phi(t)$ is applied to the ring (see text). The Be sheets are $\approx$125 μm thick. With an x-axis pseudopotential oscillation frequency $\omega_x/2\pi = 4.6$ MHz, the ion-ion spacing is approximately 3 μm.

$|\downarrow\rangle$ and $|\uparrow\rangle$, through the virtual $2p\,^2P_{1/2}$ state [5]. These beams are derived from a single laser, whose output is split by an acousto-optic modulator [8]. The beams are detuned by $\Delta/2\pi \approx 40$ GHz to the red of the $2s\,^2S_{1/2} \to 2p\,^2P_{1/2}$ transition, and their frequency difference is tuned around the $2s\,^2S_{1/2}$ hyperfine splitting of $\omega_0/2\pi \approx 1.25$ GHz. (Here, ω_0 includes stable shifts of a few megahertz from the Zeeman and ac Stark effects.) R2 is directed along $(-1/\sqrt{2})\hat{\mathbf{x}} + (1/2)(-\hat{\mathbf{y}} + \hat{\mathbf{z}})$. If R1 $\perp$ R2 as in Fig. 2, then the Raman beam wave vector difference $\boldsymbol{\delta k} \parallel \hat{\mathbf{x}}$, and the transitions are sensitive to ion motion only in this direction. If, however, R1 is counterpropagating to R2, the transitions become sensitive to motion in all three dimensions.

When two cold ions are held in the trap and undergo small oscillations about their equilibrium positions, we may solve the equations of motion using normal mode coordinates. For two ions lying along the x axis there are two modes involving motion along this axis: the center-of-mass (COM) mode (in which the ions move together with frequency $\omega_{\mathrm{COM}} = \omega_x$) and the stretch mode (wherein the ions move out of phase, with frequency $\omega_{\mathrm{str}} = \sqrt{3}\,\omega_{\mathrm{COM}}$). The other motional frequencies are ω_y (y center of mass), ω_z (z center of mass), $\sqrt{\omega_y^2 - \omega_x^2}$ (xy rocking), and $\sqrt{\omega_z^2 - \omega_x^2}$ (xz rocking).

The lower traces in Fig. 3, taken with $\boldsymbol{\delta k} \parallel \hat{\mathbf{x}}$, show an x-axis normal mode spectrum; results for the y and z modes are very similar. We take the data with the following steps: first we turn on beams D1, D2, and D3 for approximately 10 μs to Doppler cool the ions to the Lamb-Dicke regime, where the ions' confinement is much smaller than the laser wavelength. Next, we turn off beam D2, and leave beams D1 and D3 on for 5 μs to optically pump both ions to the $|\downarrow\rangle$ state. We then turn on only the Raman beams R1 and R2 for a time t_{pr}, with relative detuning $\omega_0 + \delta_{\mathrm{pr}}$ (the "Raman probe" pulse). Finally, we drive the cycling transition with D2 and measure the ions' fluorescence. We repeat the experiment at a rate of a few kilohertz while slowly sweeping δ_{pr}. If the Raman beam difference frequency is resonant with a transition, then an ion is driven from $|\downarrow\rangle \to |\uparrow\rangle$ and the D2-driven fluorescence rate drops.

For a *single* ion, the carrier transition ($\delta_{\mathrm{pr}} = 0$) causes the population to undergo sinusoidal Rabi oscillations between $|\downarrow\rangle$ and $|\uparrow\rangle$ [9]. The effective Rabi frequency is $\Omega = g_1 g_2/\Delta \approx 2\pi \times 250$ kHz, where g_1, g_2 are the single-photon resonant Rabi frequencies of beams R1 and R2. (We assume $\Delta \gg \gamma, \omega_m \gg \Omega$, where ω_m is the frequency of the motional mode of interest.) If $\delta_{\mathrm{pr}} = -\omega_x$ (the first lower x sideband), then the transition couples the states $|\downarrow, n_x\rangle$ and $|\uparrow, n_x - 1\rangle$, where n_x is the vibrational level of the quantized motion along $\hat{\mathbf{x}}$. In the Lamb-Dicke regime, the corresponding Rabi frequency is given by $\Omega_{n_x,n_x-1} = \eta_x\sqrt{n_x}\,\Omega$ [9]. Here, $\eta_x = x_0|\boldsymbol{\delta k}\cdot\hat{\mathbf{x}}|$ is the Lamb-Dicke parameter ($= 0.23$ when $\omega_x/2\pi = 8.6$ MHz) and $x_0 = \sqrt{\hbar/(2m\omega_x)}$ is the spread of the $n_x = 0$ wave function, with m being the ion's mass). (Note that if the ion is in the $n_x = 0$ state of motion, this lower sideband vanishes.) The first upper x sideband transition ($\delta_{\mathrm{pr}} = +\omega_x$) couples $|\downarrow, n_x\rangle$ and $|\uparrow, n_x + 1\rangle$ with Rabi frequency $\Omega_{n_x,n_x+1} = \eta_x\sqrt{n_x + 1}\,\Omega$.

In the case of *two* ions driven on the carrier transition, each ion independently undergoes Rabi oscillations

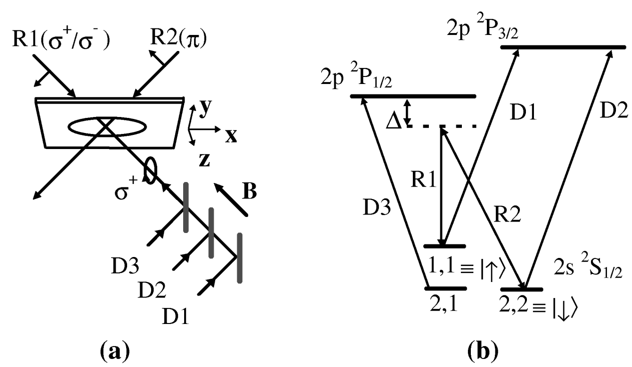

FIG. 2. (a) Laser beam geometry. The trap ring electrode is shown rotated 45° out of the page. The end cap electrodes are omitted for clarity (see Fig. 1). A magnetic field $\mathbf{B}$ of magnitude 0.2 mT defines the quantization axis along $-(1/\sqrt{2})\hat{\mathbf{x}} + (1/2)(\hat{\mathbf{y}} - \hat{\mathbf{z}})$, and laser beam polarizations are indicated. (b) Relevant $^9Be^+$ energy levels (not to scale), indicated by F, m_F quantum numbers in the ground state. ^2P fine structure splitting is $\approx$197 GHz, $^2S_{1/2}$ hyperfine splitting is $\omega_0/2\pi \approx 1.25$ GHz, $2P_{1/2}$ hyperfine splitting is $\approx$237 MHz, and the $^2P_{3/2}$ hyperfine structure ($\ll \gamma/2\pi \approx 19.4$ MHz) is not resolved. All optical transitions are near $\lambda \approx 313$ nm, and $\Delta/2\pi \approx 40$ GHz.

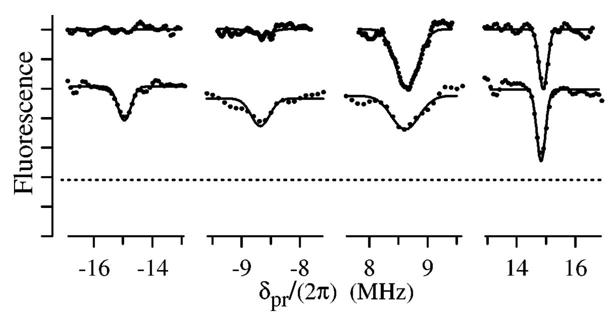

FIG. 3. Spectrum of sidebands due to two-ion x-axis normal mode motion: (from left to right) lower stretch, lower COM, upper COM, and upper stretch. The ordinate is the detuning of the Raman probe beam difference frequency from the carrier transition. The abscissa shows the ion fluorescence (proportional to the expectation value of the number of atoms in the state $|\downarrow\rangle$), plus a constant background (whose approximate level for the lower curves is indicated by the dashed line). The solid lines, meant as guides to the eye, are fits to Gaussians. The lower traces show the effects of Doppler cooling. The upper traces, offset vertically for clarity, show the effects of several pulses of Raman cooling on the mode which is displayed. Vanishing lower motional sidebands indicate cooling to the ground state of motion. The peak widths are consistent with the Raman probe pulse lengths ($\approx$3 μs).

between $|\downarrow\rangle$ and $|\uparrow\rangle$ with Rabi frequency Ω. Since the laser beam waists ($\approx 20\ \mu$m) are much larger than the ion-ion separation ($\approx 2\ \mu$m), the ions are equally illuminated. Nonetheless, if the micromotion of the two ions is different, then the reduction of the carrier (and sideband) transition strengths due to the micromotion will give a different Rabi frequency for each ion [7,10]. This could be used as a means of selectively addressing the ions [11]; however, in the present work the two ions' Rabi frequencies were equal.

Since the sideband transitions affect the motional state, which is a shared property of both ions, such transitions produce entanglement between the ions' spins and their collective motion [12]. The system can no longer be treated as two, independent, two-level systems and the measured fluorescence following the Raman probe is a complicated function of the probe pulse duration t_{pr}. For example, given an initial state $|\downarrow,\downarrow,n\rangle$ (where n is the vibrational level of the COM or stretch motion along the x axis) driven on the corresponding lower sideband for a time t_{pr}, the wave function evolves as

$$|\psi_n(t_{\mathrm{pr}})\rangle = \left\{1 - \frac{n}{2n-1}[1-\cos(Gt_{\mathrm{pr}})]\right\}|\downarrow,\downarrow,n\rangle - ie^{i(\theta-\phi)/2}\sqrt{\frac{n}{2n-1}}\sin(Gt_{\mathrm{pr}})\frac{(|\downarrow,\uparrow\rangle \pm e^{i\phi}|\uparrow,\downarrow\rangle)|n-1\rangle}{\sqrt{2}}$$
$$\mp e^{i\theta}\frac{\sqrt{n^2-n}}{2n-1}[1-\cos(Gt_{\mathrm{pr}})]|\uparrow,\uparrow,n-2\rangle, \quad (1)$$

where $G = \sqrt{2(2n-1)}\,\Omega\,\eta_{x,m}$ and θ, ϕ are the sum and difference of the Raman beam phases at the ions. On the COM sideband [top sign in Eq. (1)], $\eta_{x,m} = \eta_{x,\mathrm{COM}} = \eta_x/\sqrt{2}$ (down by a factor of $\sqrt{2}$ from the single-ion case due to the extra mass of the two-ion string), whereas on the stretch sideband (lower sign), $\eta_{x,m} = \eta_{x,\mathrm{str}} = \eta_x/\sqrt{2\sqrt{3}}$. The expressions for transitions on the upper motional sidebands are similar. If, before the Raman probe pulse, the ions have probability p_n of being in the motional state $|n\rangle$, the subsequently measured average fluorescence from the cycling transition is

$$S(t_{\mathrm{pr}}) = \sum_n p_n(2|\langle\downarrow,\downarrow,n|\psi_n(t_{\mathrm{pr}})\rangle|^2 + |\langle\downarrow,\uparrow,n-1|\psi_n(t_{\mathrm{pr}})\rangle|^2 + |\langle\uparrow,\downarrow,n-1|\psi_n(t_{\mathrm{pr}})\rangle|^2)\,. \quad (2)$$

This signal is proportional to the expectation value of the number of atoms in the state $|\downarrow\rangle$. For the data shown in Fig. 3, t_{pr} was chosen to maximize the sideband features.

The upper traces in Fig. 3 show the effects of adding several cycles of Raman cooling [5] on one particular x mode after the Doppler cooling but before the probe pulse. The reduction in the mean vibrational number $\langle n\rangle$ is indicated by the reduction in size of the lower sideband, which vanishes in the limit $\langle n\rangle \rightarrow 0$. The data are consistent with a thermal state of $\langle n_{\mathrm{COM}}\rangle = 0.11^{+0.17}_{-0.03}$ or $\langle n_{\mathrm{str}}\rangle = 0.01^{+0.08}_{-0.01}$. This implies that the COM and stretch modes are in their ground states 90^{+3}_{-12}% and 99^{+1}_{-7}% of the time, respectively. We have also *simultaneously* cooled the COM and stretch modes along x, to comparable values of $\langle n\rangle$ (and have separately cooled the other four motional modes—y and z COM, xy rocking, and xz rocking—to near their ground states).

Each cycle of Raman cooling consists of (i) a pulse of the Raman beams with their difference frequency tuned to one of the lower sidebands (COM or stretch mode) and (ii) optical repumping to the $|\downarrow\rangle$ state driven by beams D1 and D3. The Raman transition reduces the vibrational energy by $\hbar\omega_m$, whereas the repumping, on average, heats each mode by approximately the recoil energy ($\ll\hbar\omega_m$). Therefore, the ion is cooled through this process. Five pulses of Raman cooling were used for the data shown in Fig. 3. The exact durations of the Raman pulses were chosen to optimize the cooling rate—each pulse was approximately 5 μs long.

For an ion-trap implementation of a quantum computer, the motional modes are most susceptible to decoherence. The ions' motional states lose coherence if they couple to (stochastic) electric fields caused by fluctuating potentials on the electrodes. This leads to heating, which has previously been observed in single ions [5,10,13]; in Ref. [5], the heating drove the ion out of the motional (COM) ground state in approximately 1 ms. We have performed similar heating measurements on the COM and non-COM modes of motion of two ions. The results are summarized in Table I. The heating rate was determined by inserting a delay between laser cooling and the Raman

TABLE I. Heating rates of the six normal modes of two trapped ions. The Raman beams were counterpropagating for the y- and z-axis data, making the Raman probe sensitive to motion in all three dimensions. Note that the COM modes are heated at a much higher rate than the non-COM modes (see text). (The precision with which the heating rates are given for the last five modes is limited by measurement noise.)

Mode	$\omega_m/2\pi$ (MHz)	$\delta\langle n\rangle/\delta t$ (ms^{-1})
x_{COM}	8.6	19^{+40}_{-13}
y_{COM}	17.6	>10
z_{COM}	9.3	>20
x_{str}	14.9	<0.18
xy_{rocking}	15.4	<1
xz_{rocking}	3.6	<0.5

probe. The main results from these data are that the COM modes are heated out of the ground state much more quickly than the non-COM modes. This can be explained as follows.

The COM modes, in which both ions move in phase, can be excited by a uniform electric field. However, no non-COM mode can be excited by a uniform electric field [14]—since these modes involve *differential* motion of the ions, they can be driven only by field gradients. If the fluctuating field at the ion (along the direction of motion of the mode of interest) is $E(t)$, an estimate of the corresponding field gradient is $E(t)/d$, where d is a characteristic internal dimension of the trap. For stochastic fields, the COM heating rate scales as $\langle E^2(t)\rangle$; the non-COM mode heating rates scale as $\langle[\frac{E(t)}{d}\Delta x]^2\rangle$ (where Δx is the ion-ion separation), down by a factor of 10^4 for the present trap. Similarly, other non-COM modes for more than two ions can be excited only by higher-order field gradients, leading to further reductions in their heating.

This suggests using non-COM modes for the quantum data bus in the Cirac-Zoller scheme. Excitation of the "spectator" COM modes along the direction to which the Raman transitions are sensitive will still alter the Rabi frequencies, but these effects will be higher order in the Lamb-Dicke parameter [10]. In the two-ion example, in the Lamb-Dicke regime, the Rabi frequency for a first sideband transition $|n_1\rangle \rightarrow |n_1'\rangle$ on (cold) mode 1, given that (hotter) mode 2 is in the state $|n_2\rangle$, is [10]

$$\Omega_{n_1,n_1'}(n_2) = \Omega\,\eta_1\sqrt{n_{1>}}\,e^{-(\eta_1^2+\eta_2^2)/2}(1 - n_2\eta_2^2)\,, \quad (3)$$

where $n_{1>}$ denotes the larger of n_1' or n_1, and η_1 and η_2 are the Lamb-Dicke parameters for modes 1 and 2, respectively. Fluctuations in the Rabi frequency of mode 1 due to fluctuations in n_2 therefore occur in order η_2^2. However, for the conditions of the present experiment, even if quantum logic operations were performed using the x-stretch mode, the x-COM mode heating would still limit the number of operations to around ten by the above mechanism. Clearly, this heating must be eliminated in future experiments.

The two-ion cooling results presented here are comparable to our previous single-ion results [5], indicating that rf heating should not be a concern for small numbers of ions [10]. Comparable cooling for $N > 2$ ions should not present any fundamental difficulties, as long as spurious overlaps of motional modes are avoided.

The preparation of a pure state of motion (the ground state) of multiple trapped ions represents the first step towards realizing quantum logic operations on them. Such operations should lead to the creation of arbitrary entangled states of massive particles, including EPR- or GHZ-like spin states [15]. Unlike other systems in which EPR states have been generated, it should be possible to reliably create these states on demand [11] rather than by a selection process, and to detect them with nearly perfect efficiency [16].

We acknowledge support from the U.S. National Security Agency, Office of Naval Research, and Army Research Office. We thank Kristan Corwin, David Kielpinski, and Matt Young for critical readings of the manuscript.

*Electronic address: kingb@ucsu.Colorado.EDU
†Present address: Institut für Experimentalphysik, Universität Innsbruck, Innsbruck, Austria.

[1] A. Ekert and R. Jozsa, Rev. Mod. Phys. **68**, 733 (1996); A. Steane, Rep. Prog. Phys. **61**, 117 (1998).
[2] J. I. Cirac and P. Zoller, Phys. Rev. Lett. **74**, 4091 (1995).
[3] If the "data bus" is in a thermal state with probability P_0 of being in the ground state then, if we ignore all other sources of error, a given quantum computation must be repeated $1/P_0$ times, on average, to give a correct answer.
[4] C. Monroe *et al.*, Phys. Rev. Lett. **75**, 4714 (1995).
[5] C. Monroe *et al.*, Phys. Rev. Lett. **75**, 4011 (1995).
[6] S. R. Jefferts, C. Monroe, E. Bell, and D. J. Wineland, Phys. Rev. A **51**, 3112 (1995).
[7] C. J. Myatt *et al.*, in *Methods for Ultrasensitive Detection*, SPIE Proceedings Vol. 3270, edited by Bryan L. Fearey (SPIE–International Society for Optical Engineering, Bellingham, WA, 1998) p. 131; R. G. Devoe, Phys. Rev. A **58**, 910–914 (1998).
[8] J. E. Thomas *et al.*, Phys. Rev. Lett. **48**, 867 (1982).
[9] D. M. Meekhof *et al.*, Phys. Rev. Lett. **76**, 1796 (1996).
[10] D. J. Wineland *et al.*, J. Res. Natl. Inst. Stand. Technol. **103**, 259 (1998); Forschr. Phys. **46**, 363 (1998).
[11] Q. A. Turchette *et al.*, quant-phy/9806012.
[12] D. J. Wineland, J. J. Bollinger, W. M. Itano, and D. J. Heinzen, Phys. Rev. A **50**, 67 (1994).
[13] F. Diedrich, J. C. Bergquist, W. M. Itano, and D. J. Wineland, Phys. Rev. Lett. **62**, 403 (1989).
[14] D. J. Wineland and H. G. Dehmelt, J. Appl. Phys. **46**, 919 (1975); D. F. V. James, Phys. Rev. Lett. **81**, 317 (1998).
[15] A. Einstein, B. Podolsky, and N. Rosen, Phys. Rev. **47**, 777 (1935); D. M. Greenberger, M. A. Horne, A. Shimony, and A. Zeilinger, Am. J. Phys. **58**, 1131 (1990); M. Lamehi-Rachti and W. Mittig, Phys. Rev. D **14**, 2543 (1976); E. Hagley *et al.*, Phys. Rev. Lett. **79**, 1 (1997).
[16] R. Blatt and P. Zoller, Eur. J. Phys. **9**, 250 (1988).